

BEYOND POPULAR SCIENCE



DAVID H. SILVER



BEYOND POPULAR SCIENCE

David H. Silver

<https://www.openbookpublishers.com>

© 2026 David H. Silver



This work is licensed under the Creative Commons Attribution-NonCommercial 4.0 International (CC BY-NC 4.0). This license allows you to share, copy, distribute and transmit the text; to adapt the text for non-commercial purposes of the text providing attribution is made to the authors (but not in any way that suggests that they endorse you or your use of the work). Attribution should include the following information:

David H. Silver, *Beyond Popular Science*. Cambridge, UK: Open Book Publishers, 2026,
<https://doi.org/10.11647/OBP.0526>

Further details about CC BY-NC licenses are available at
<https://creativecommons.org/licenses/by-nc/4.0/>

Copyright and permissions for the reuse of many of the images included in this publication differ from the above. This information is provided in the captions and in the list of illustrations. Unless otherwise stated, figures are reproduced under the fair dealing principle. Every effort has been made to identify and contact copyright holders and any omission or error will be corrected if notification is made to the publisher.

All external links were active at the time of publication unless otherwise stated and have been archived via the Internet Archive Wayback Machine at
<https://archive.org/web>

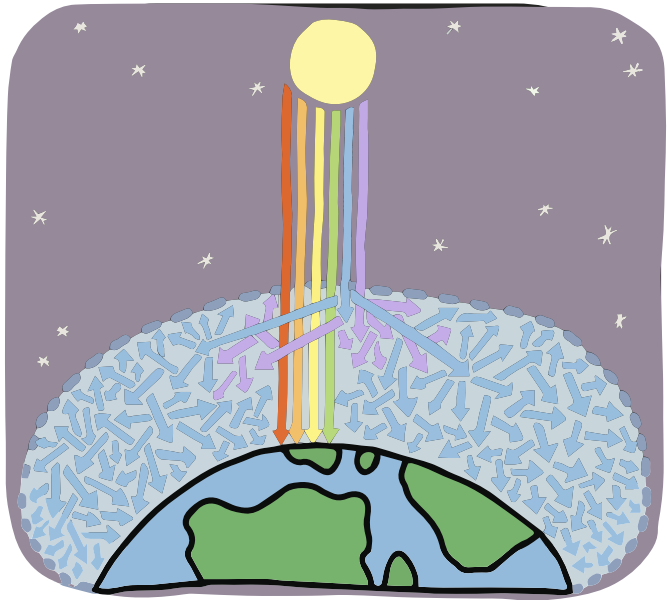
Digital material and resources associated with this volume are available at
<https://doi.org/10.11647/OBP.0526#resources>

ISBN Paperback:	978-1-80511-877-0
ISBN Hardback:	978-1-80511-878-7
ISBN Digital (PDF):	978-1-80511-879-4
ISBN HTML:	978-1-80511-881-7
ISBN Digital ebook (epub):	978-1-80511-880-0
DOI:	10.11647/OBP.0526

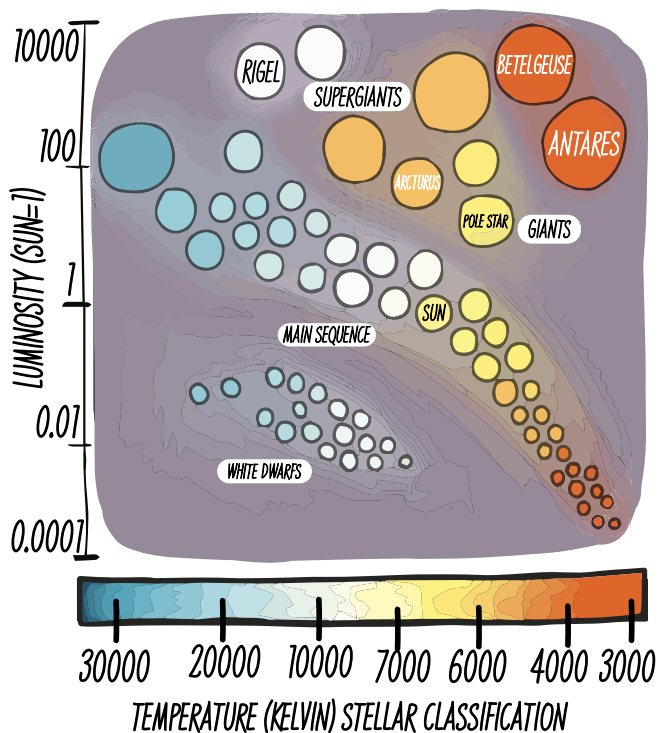
Cover image by Enny Silver and David H. Silver
Cover design by Jeevanjot Kaur Nagpal

A Spectrum of Skies

Top (Atmospheric Filtering of Stellar Radiation): Sunlight reaching Earth undergoes selective scattering by the atmosphere. Shorter wavelengths (blue, violet) are scattered in all directions, while longer wavelengths (red, orange) pass through more directly. This results in both the blue sky and the reddening of the Sun near the horizon.

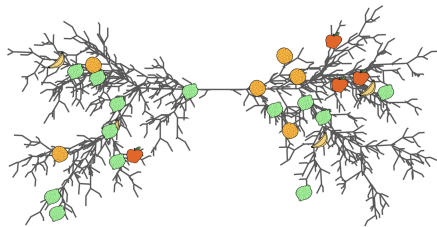


Bottom (Hertzsprung–Russell Diagram): Stars are plotted by surface temperature (x-axis, decreasing rightward) and luminosity (y-axis, log scale). Main sequence stars form a diagonal band; giants and supergiants lie above, white dwarfs below. The Sun sits in the middle of the main sequence. The temperature scale reflects stellar classification: blue-hot stars (left) are hotter and more luminous; red stars (right) are cooler.



A Spectrum of Skies

Sky colours are determined by light scattering and spectral signatures. Earth's blue sky results from Rayleigh scattering, where nitrogen and oxygen molecules preferentially scatter shorter wavelengths by factors of 10–100 times more efficiently than longer ones. Mars's butterscotch-orange haze results from suspended dust particles 1–10 micrometres across, scattering all wavelengths equally while absorbing blue light. Titan's deep orange hue comes from photochemical hazes (tholins) produced by UV irradiation of methane, while Venus's perpetual cloud deck creates brilliant white from sulfuric acid droplets.



RAYLEIGH SCATTERING λ^{-4} ◦ BLUE SKY PHYSICS ◦ MARS IRON
OXIDE ◦ VENUS SULPHURIC ACID ◦ URANUS-NEPTUNE
METHANE ◦ STELLAR TEMPERATURE COLOURS ◦ H α RED
NEBULAE ◦ INTERSTELLAR REDDENING ◦ DOPPLER COLOUR
SHIFT ◦ SPECTROSCOPY TOOL ◦ ATMOSPHERIC PATH LENGTH

“Oh, I’m sorry. Well, I could put the trash into a landfill
where it’s going to stay for millions of years,
or I could burn it up and get a nice smoky smell in here
and let that smoke go into the sky where it turns into stars.”

– Charlie Kelly

“That doesn’t sound right,
but I don’t know enough about stars to dispute it.”

– Mac

A Spectrum of Skies

The study of light dispersion and the spectral analysis of celestial objects motivates the scientific study into the nature of cosmic colour. Isaac Newton's prism experiments in the 1660s revealed that white light contains a continuous spectrum of colours, initiating the quantitative study of optics. By the early nineteenth century, Joseph von Fraunhofer's meticulous cataloguing of dark absorption lines in the solar spectrum laid the foundation for stellar spectroscopy. These lines, later identified with specific chemical elements, confirmed that stars share a common elemental makeup with Earth.

Mid-nineteenth-century advances by William Huggins and Angelo Secchi introduced systematic spectral classification and chemical identification of stars and nebulae. Secchi's grouping of stellar spectra foreshadowed the modern OBAFGKM sequence, while Huggins showed that some nebulae emit light like gases rather than collections of stars. Theoretical breakthroughs followed in the early twentieth century with Planck's and Wien's radiation laws and the rise of quantum theory, which linked spectral lines to electronic transitions within atoms.

Meanwhile, on Earth, John Tyndall's experiments on atmospheric scattering in the late nineteenth century demonstrated wavelength-dependent scattering in air (the Tyndall effect). In 1871, Lord Rayleigh formalised the underlying physics, showing that shorter wavelengths scatter more efficiently and explaining the blue sky. These ideas were extended to planetary atmospheres through spectroscopic work by Vesto Slipher in the 1910s and Gerard Kuiper in the 1940s, who linked atmospheric composition to the observed colours of planets.

With the dawn of the space age, direct observations of planetary skies became possible. NASA's Mariner, Viking, and Voyager missions collected spectral data from Mars, Venus, Jupiter, and beyond, confirming that dust, aerosols, and gases define planetary hues. In the early 2000s, Cassini's orbit of Saturn and Titan revealed complex hazes and photochemical effects shaping visible colouration. Across centuries - from Newton's spectrum to Cassini's spectrometers - the colour of the cosmos has transitioned from aesthetic impression to precise physical measurement.

The blue colour of Earth's sky results from the interaction of solar radiation with atmospheric gases. When sunlight enters the atmosphere, air molecules scatter it in multiple directions, creating a diffuse background of illumination that makes the sky appear bright when the Sun is not in direct view. This scattering process depends on wavelength: when the scattering particles are much smaller than the wavelength of light, as air molecules are, the scattering cross-section varies inversely with the fourth power of wavelength. This λ^{-4} dependence arises because small particles respond to electromagnetic waves as induced oscillating dipoles—the passing light wave causes electrons to oscillate, and these accelerating charges radiate energy in all directions. The power radiated by an oscillating dipole scales with the fourth power of its oscillation frequency, which translates to the fourth power of wavelength in the denominator. This phenomenon, known as Rayleigh

scattering (Rayleigh, 1871), favours shorter-wavelength light, such as blue and violet, over longer-wavelength light, such as red.

Although violet light scatters more efficiently than blue, the sky appears blue rather than violet due to two compensating factors: human eyes are less sensitive to violet wavelengths, and the solar spectrum itself contains slightly less energy in the violet band. At sunrise and sunset, the geometry changes. Sunlight must traverse a much longer path through the atmosphere—up to forty times the distance at noon—causing blue and green wavelengths to scatter away before reaching observers, leaving predominantly red and orange light to paint the horizon.

Perceived colour corresponds to measurable differences in scattering efficiency and atmospheric path length, arising from electromagnetic interactions between photons and molecules. The same mechanisms of scattering, absorption, and emission operate throughout astronomical systems. Whenever light interacts with matter, whether gas, dust, or solid surfaces, its spectrum undergoes alterations that depend on the physical properties of the medium. These spectral changes manifest as both broad redistributions of intensity across wavelengths and selective suppression or enhancement of specific bands, encoding temperature, chemical composition, and geometric configuration in the spectrum. Colour in astronomy is a quantitative tool—a compressed summary of the integrated intensity distribution across wavelength bands.

Unlike planets, stars generate their own light through thermal radiation, with each star approximating a blackbody whose emission spectrum depends primarily on surface temperature. As temperature increases, Wien's displacement law (Wien, 1896) dictates that the peak emission shifts to shorter wavelengths: the hottest O-type stars blaze at 30,000 K with peak emission in the ultraviolet, while cool M-dwarfs at 3,000 K peak in the infrared. Our Sun, at approximately 5,800 K, emits across the visible spectrum with peak intensity in the green, though the integrated light appears white-yellow when viewed through Earth's atmosphere. The stellar classification sequence—O, B, A, F, G, K, M—encapsulates both this temperature progression and the changing patterns of absorption lines that appear as different atomic species become ionised or excited in stellar atmospheres of varying temperature.

The colours we observe in stars reflect their physical state at multiple scales. Surface gravity affects spectral line profiles—giant stars show narrower absorption lines than dwarfs of the same temperature due to lower atmospheric pressure. Metallicity alters colour subtly: metal-poor stars appear bluer than metal-rich stars at the same temperature because metals provide additional opacity in the blue and ultraviolet. Rapid rotation produces gravity darkening: equators are cooler and dimmer while poles are hotter and brighter (von Zeipel effect) (von Zeipel, 1924), leading to colour and brightness gradients across rapidly spinning stars such as Vega.

Stellar atmospheres contain molecules that create distinctive colour signatures. Cool stars below 3,500 K form titanium oxide (TiO), whose broad absorption bands define the M spectral class and create deep red colours. Carbon stars form carbon compounds instead, appearing distinctly crimson. S-type stars show zirconium oxide bands, while the coolest L and T dwarfs—discovered only through infrared surveys—contain methane and water

vapour, rendering them invisible to the naked eye despite being closer than many visible stars.

Variable stars demonstrate colour as a dynamic property. Cepheid variables pulsate radially, their surfaces cooling and reddening during expansion, then heating and becoming bluer during contraction. RR Lyrae stars, a type of variable star, cycle through colour changes in hours rather than days. Mira variables—long-period pulsating giants—can shift from orange to deep red over months as their radii double. These colour variations serve as cosmic distance indicators at ranges beyond the direct reach of parallax, with period–luminosity relationships (Leavitt & Pickering, 1912) calibrated using colour information and reddening corrections.

Interstellar reddening complicates stellar colour interpretation. Dust grains preferentially scatter blue light, making distant stars appear redder than their intrinsic colours—a phenomenon distinct from cosmological redshift. The amount of reddening depends on grain size distribution and composition along the line of sight. Astronomers must correct for this extinction to determine true stellar properties. Some regions show anomalous extinction curves where ultraviolet absorption exceeds predictions, suggesting unusual dust compositions possibly formed in supernova ejecta or stellar winds.

Planets reflect sunlight, with apparent colour determined by the interplay between surface reflectivity and atmospheric absorption. Mars owes its rusty appearance to iron oxide in its regolith, which reflects red wavelengths while absorbing blue and green. This selective reflection creates the planet's reddish hue that persists across all viewing angles and seasons. Jupiter presents a more complex palette: its banded appearance results from layered cloud structures at different altitudes, with white ammonia ice clouds at higher levels and darker, reddish-brown clouds containing complex organic chromophores at greater depths.

The ice giants Uranus and Neptune share a different colouring mechanism. Both possess methane in their upper atmospheres, which absorbs red light beyond 600 nanometres while allowing blue wavelengths to scatter back to space. Yet Neptune appears a deeper, more vivid blue despite similar methane concentrations. Neptune's atmospheric dynamics differ: Neptune's more active vertical mixing clears high-altitude hydrocarbon hazes that would otherwise dilute the pure blue colour, while Uranus retains a whitish haze layer that mutes its appearance.

Beyond planetary atmospheres, interstellar nebulae paint the cosmos with characteristic colours. Emission nebulae glow with the light of ionised gas, powered by nearby hot stars whose ultraviolet radiation strips electrons from atoms. The dominant spectral signature is the $H\alpha$ line of hydrogen at precisely 656.3 nanometres, creating the deep red glow of star-forming regions such as Orion. Planetary nebulae add complexity to this palette through doubly ionised oxygen ([OIII]) emission near 500 nanometres, producing ethereal blue-green shells around dying stars.

Reflection nebulae consist of interstellar dust clouds that scatter light from nearby stars. Like Earth's atmosphere, they scatter blue light more efficiently than red. The result is a delicate blue illumination surrounding young, hot stars, even though the dust grains themselves emit no light. In contrast, dark nebulae represent the universe's silhouettes—dense molecular

clouds so opaque they block background starlight entirely, appearing as sharply defined voids against the stellar backdrop, such as the famous Horsehead Nebula.

On the grandest scales, entire galaxies display integrated colours that chronicle their stellar populations and evolutionary histories. A galaxy's colour represents the combined light of billions of stars, weighted heavily toward the brightest members. In spiral galaxies with active star formation, massive O and B type stars dominate the integrated light despite comprising less than 1% of the total stellar population. These stellar giants burn so brilliantly that they outshine thousands of Sun-like stars, lending spiral arms their blue-white glow. Elliptical galaxies, having exhausted their gas reserves billions of years ago, harbour predominantly old, cool stars that together produce a golden or reddish cast.

Interstellar dust modifies galactic colours through extinction—the wavelength-dependent absorption and scattering that removes blue light from our line of sight. Edge-on spiral galaxies show dark dust lanes bisecting their discs and reddening the light from stars behind them, much as Earth's atmosphere reddens the setting Sun.

Colour in astronomy extends beyond intrinsic properties to include the effects of motion through the Doppler shift. When celestial objects move relative to observers, their spectrum shifts: approaching objects compress wavelengths toward the blue, while receding objects stretch them toward the red. For nearby stars and galaxies, these shifts measure radial velocities—the component of motion along our line of sight. Cosmological redshift occurs as the expansion (Hubble, 1929) of intergalactic space stretches light waves during their journey across the universe, with the amount of stretching depending on both distance and the universe's expansion history.

Modern astronomical imaging translates physical phenomena into visual representations through colour-coding schemes. True-colour images approximate human vision by combining exposures through red, green, and blue filters matched to our eye's sensitivity. False-colour imaging employs colours as a visualisation tool for invisible wavelengths. Radio telescopes might encode intensity as red, X-ray telescopes as blue, and infrared as green, creating composite images that reveal hidden structures. Narrow-band filters isolate specific emission lines—hydrogen-alpha, oxygen-III, sulphur-II—each mapped to different colours to highlight ionisation zones, shock fronts, and chemical gradients. Colour mapping displays temperature distributions, velocity fields, and magnetic structures across cosmic scales.

Transmitted wavelengths broadcast physical processes throughout the cosmos. Every hue we measure corresponds to specific interactions between electromagnetic radiation and matter: Rayleigh scattering in atmospheres, thermal emission from stellar surfaces, electronic transitions in nebular gas, or the cosmic expansion detected in galactic redshifts. These mechanisms—absorption, scattering, emission, and Doppler shifting—operate according to known physical theories, making the universe into a vast spectroscopic laboratory where colour reveals temperature, composition, motion, and history across scales from planetary atmospheres to galaxy clusters.

Why This Story

This was one of the first chapters I wrote. I wanted a more sophisticated answer to a question children often ask: why is the sky blue? Why is the Sun red at sunset? I knew the basic explanation—Rayleigh scattering and wavelength dependence—but I wanted a version that would remain meaningful even after they learned mathematics and a bit of science. The question becomes more, not less, interesting with each layer of generalisation: from sunlight and air to blackbody curves, stellar classifications, and interstellar dust. Writing this chapter helped establish the book's tone—clear, complex, physically grounded—and set the standard for treating simple questions with full scientific seriousness.



Nine simulated daytime skies from each planet in the Solar System, arranged heliocentrically around the Sun in a 3×3 grid. The rows (left to right, top to bottom) correspond to: Mercury, Venus, Earth; Mars, Sun, Jupiter; Saturn, Uranus, Neptune. Each panel reflects sky colour, atmospheric scattering, and visible celestial features such as moons, rings, and the Sun's apparent size, as modelled for surface or high-atmosphere observation.

Quantitative Analysis of Astronomical Colour

Radiative Transfer and Blackbody Radiation

The propagation of specific intensity I_ν along a path s is governed by the equation of radiative transfer:

$$\frac{dI_\nu}{ds} = j_\nu - \alpha_\nu I_\nu - \sigma_\nu I_\nu + \iint \sigma_\nu(\Omega', \Omega) I_\nu(\Omega') d\Omega',$$

where j_ν is the emission coefficient, α_ν is the absorption coefficient, and σ_ν is the scattering coefficient. The optical depth is $d\tau_\nu = (\alpha_\nu + \sigma_\nu) ds$. In local thermodynamic equilibrium (LTE) without scattering, the source function reduces to $S_\nu = j_\nu/\alpha_\nu$, which approaches the Planck function for thermal emission. With scattering present, the total source function mixes thermal emission and angle-averaged scattered intensity: $S_\nu = (\alpha_\nu B_\nu + \sigma_\nu J_\nu)/(\alpha_\nu + \sigma_\nu)$, where J_ν is the mean intensity.

$$B_\nu(T) = \frac{2h\nu^3}{c^2} \left[\exp\left(\frac{h\nu}{kT}\right) - 1 \right]^{-1}.$$

The wavelength of peak emission is given by Wien's law:

$$\lambda_{\max} T = b \approx 2.898 \times 10^{-3} \text{ m} \cdot \text{K}$$

and the total emitted flux per unit area follows the Stefan-Boltzmann law:

$$F = \sigma T^4, \quad \sigma = \frac{2\pi^5 k^4}{15c^2 h^3}.$$

Stellar temperatures can be inferred by fitting observed continua or via colour indices (e.g., $B - V$), which measure differences in magnitude across filtered bands.

Spectral Lines and Atmospheric Composition

Spectral lines originate from electronic transitions with energy $\Delta E = h\nu = E_u - E_l$. In LTE, population ratios follow the Boltzmann distribution:

$$\frac{N_u}{N_l} = \frac{g_u}{g_l} \exp\left(-\frac{E_u - E_l}{kT}\right).$$

Ionization states are governed by the Saha equation:

$$\frac{N_{i+1} N_e}{N_i} = \frac{2g_{i+1}}{g_i} \left(\frac{2\pi m_e kT}{h^2}\right)^{3/2} \exp\left(-\frac{\chi_i}{kT}\right)$$

where χ_i is the ionisation energy and N_e is the electron density. Line shapes are broadened by natural width, thermal Doppler broadening:

$$\Delta\lambda_D = \lambda_0 \left(\frac{2kT}{mc^2}\right)^{1/2}$$

and collisional (pressure) broadening, which scales with density. Observed line intensities allow reconstruction of chemical abundances and physical conditions.

Motion, Redshift, and Extinction

The Doppler effect shifts wavelengths by

$$\frac{\Delta\lambda}{\lambda_0} = \frac{v_r}{c}, \quad (v_r \ll c)$$

where v_r is the radial velocity. Redshift ($\Delta\lambda > 0$) indicates recession; blueshift indicates approach. For distant galaxies, the cosmological redshift z is related to the scale factor $R(t)$ via $1+z = R(t_{\text{obs}})/R(t_{\text{emit}})$ and follows Hubble's law for $z \ll 1$: $v = H_0 d$.

Extinction by dust is quantified by

$$A_\lambda = 1.086 \tau_\lambda = -2.5 \log_{10} (F_\lambda/F_{\lambda,0})$$

where τ_λ is the optical depth. Reddening is the differential extinction between bands:

$$E(B - V) = A_B - A_V$$

and the total-to-selective extinction ratio $R_V = A_V/E(B - V)$ typically has a value near 3.1 for the diffuse interstellar medium. For small particles $a \ll \lambda$, Rayleigh scattering dominates, with efficiency $\propto \lambda^{-4}$. For $a \sim \lambda$, Mie scattering applies, with weaker wavelength dependence.

References:

- Rybicki, G. B., and Lightman, A. P. (1979). *Radiative Processes in Astrophysics*. Wiley.
 Draine, B. T. (2003). *Interstellar Dust Grains. Annual Review of Astronomy and Astrophysics*.

